Hyperonic Three-Body Forces & Neutron Stars

Isaac Vidaña
CFC, University of Coimbra

Hypernuclear Workshop
May 27th – 29th 2014, Jefferson Lab
Newport News, VA (USA)

This study is part of the Ph.D. Thesis of Domenico Logoteta (Univ. Coimbra, 2013)

in collaboration also with

C. Providência

A. Polls

I. Bombaci

Some known facts about Neutron Stars

- Formed in: type II, Ib or Ic SN
- Mass: $M \sim 1 - 2\ M_{\odot}$
- Radius: $R \sim\ 10 - 12$ km
- Density: $\rho \sim 10^{14} - 10^{15}\ g/cm^3$

$\rho_{universe} \sim\ 10^{-30}\ g/cm^3$

$\rho_{sun} \sim\ 1.4\ \ g/cm^3$

$\rho_{earth} \sim\ 5.5\ \ g/cm^3$

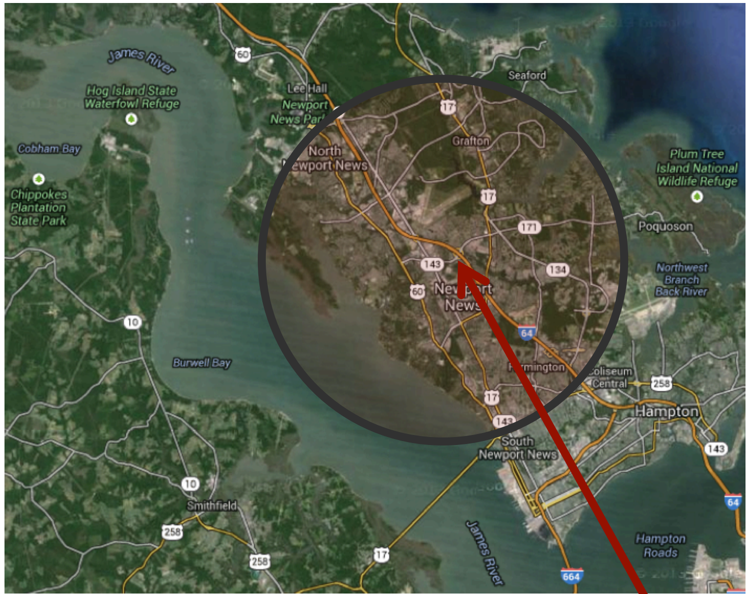

You are here !!

- Baryonic number: $N_b \sim 10^{57}$ (“giant nuclei”)
- Magnetic field: $B \sim 10^{8\ldots15}$ G ($10^{4\ldots11}$ T)

$0.3 - 0.5G$

Earth

$10^3 - 10^4 G$

Magnet

$10^5 G$

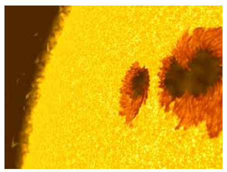

Sunspots

$4.5x10^5 G$

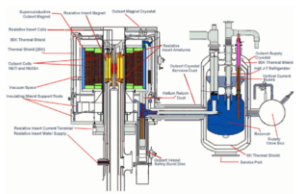

Largest continuous field in lab. (FSU, USA)

$2.8x10^7 G$

Largest magnetic pulse in lab. (Russia)

- Electric field: $E \sim 10^{18}$ V/cm

- Temperature: $T \sim 10^{6\ldots11}$ K

- Rotational period distribution
  ➔ two types of pulsars:

    - pulsars with P ~ s
    - pulsars with P ~ ms

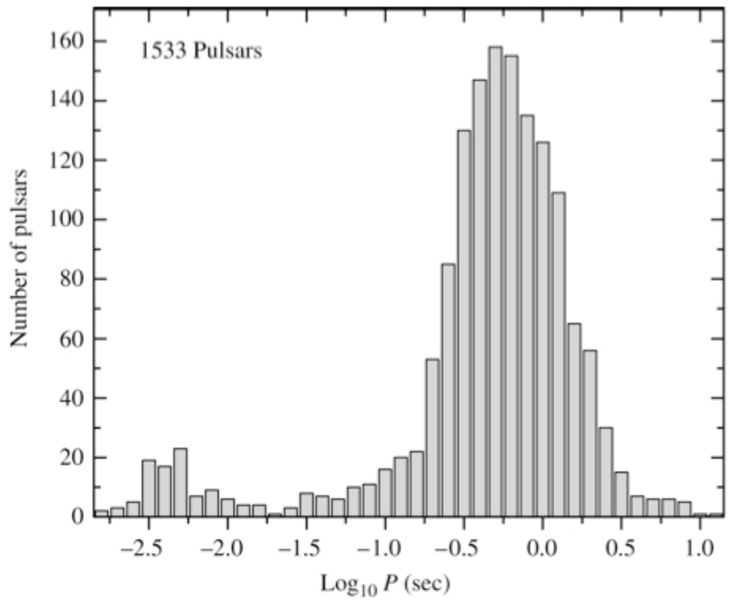

Shortest rotational period PSR in Terzan 5: $P_{J1748\text{-}2446ad} = 1.39$ ms

- Accretion rates: 10^{-10} to 10^{-8} $M_{\odot}$/year

Anatomy of a Neutron Star

Equilibrium composition determined by

✓ Charge neutrality

$$\sum_i q_i \rho_i = 0$$

✓ Equilibrium with respect to weak interacting processes

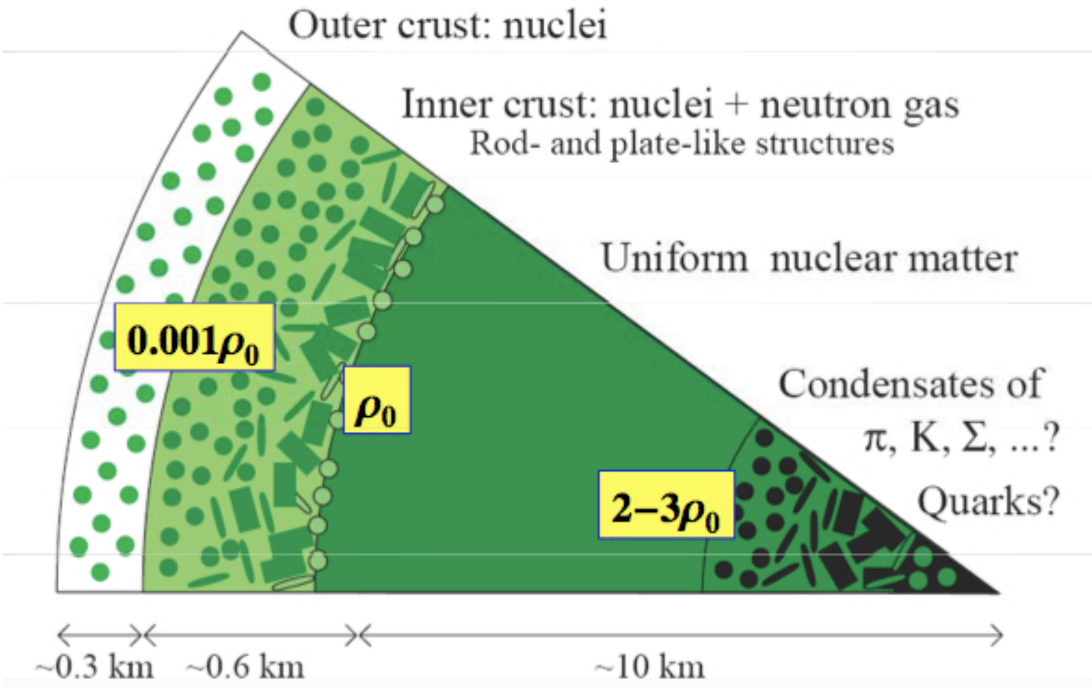

$$b_1 \rightarrow b_2 + l + \bar{\nu}_l$$
$$b_2 + l \rightarrow b_1 + \nu_l$$

$$\longrightarrow \quad \mu_i = b_i \mu_n - q_i \left(\mu_e - \mu_{\nu_e} \right), \quad \mu_i = \frac{\partial \varepsilon}{\partial \rho_i}$$

Hyperons in Neutron Stars

Hyperons in NS considered by many authors since the pioneering work of Ambartsumyan & Saakyan (1960)

Phenomenological approaches

- Relativistic Mean Field Models: Glendenning 1985; Knorren et al. 1995; Shaffner-Bielich & Mishustin 1996, Bonano & Sedrakian 2012, …
- Non-realtivistic potential model: Balberg & Gal 1997
- Quark-meson coupling model: Pal et al. 1999, …
- Chiral Effective Lagrangians: Hanauske et al., 2000
- Density dependent hadron field models: Hofmann, Keil & Lenske 2001

Microscopic approaches

- Brueckner-Hartree-Fock theory: Baldo et al. 2000; I. V. et al. 2000, Schulze et al. 2006, I.V. et al. 2011, Burgio et al. 2011, Schulze & Rijken 2011
- DBHF: Sammarruca (2009)
- $V_{\text{low k}}$: Djapo, Schaefer & Wambach, 2010

Sorry if I missed somebody

Hyperons are expected to appear in the core of neutron stars at $\rho \sim (2\text{-}3)\rho_0$ when μ_N is large enough to make the conversion of N into Y energetically favorable.

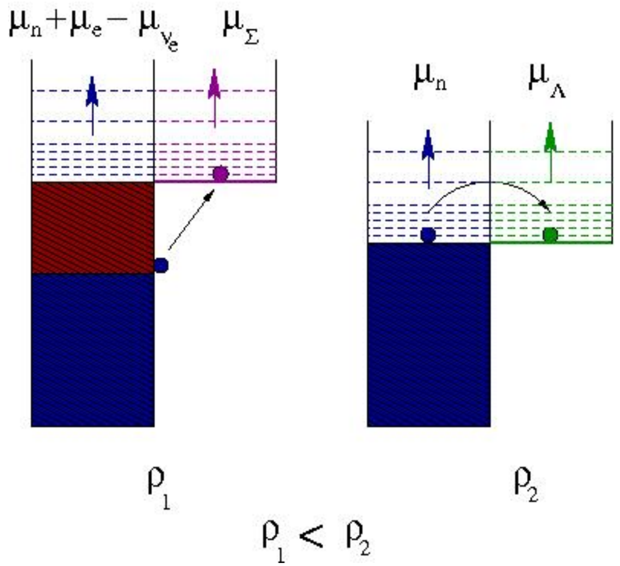

$$\mu_{\Sigma^-} = \mu_n + \mu_{e^-} - \mu_{\nu_{e^-}}$$

$$\mu_\Lambda = \mu_n$$

$$n + n \rightarrow n + \Lambda$$

$$p + e^- \rightarrow \Lambda + \nu_{e^-}$$

$$n + n \rightarrow p + \Sigma^-$$

$$n + e^- \rightarrow \Sigma^- + \nu_{e^-}$$

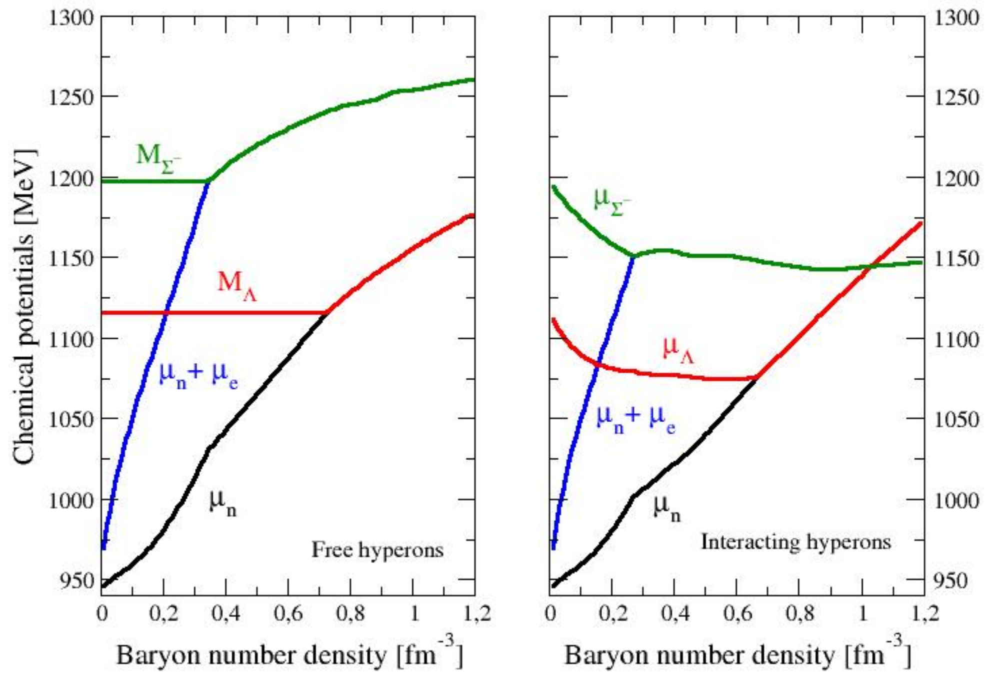

Effect of Hyperons in the EoS and Mass of Neutron Stars

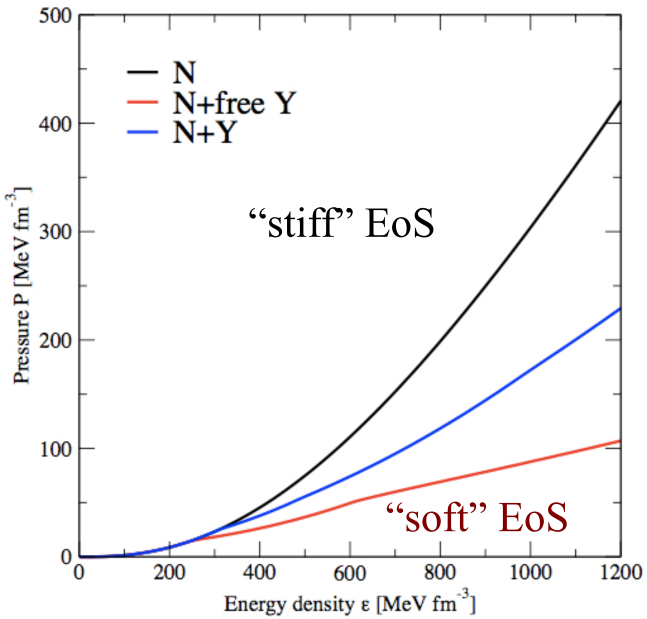

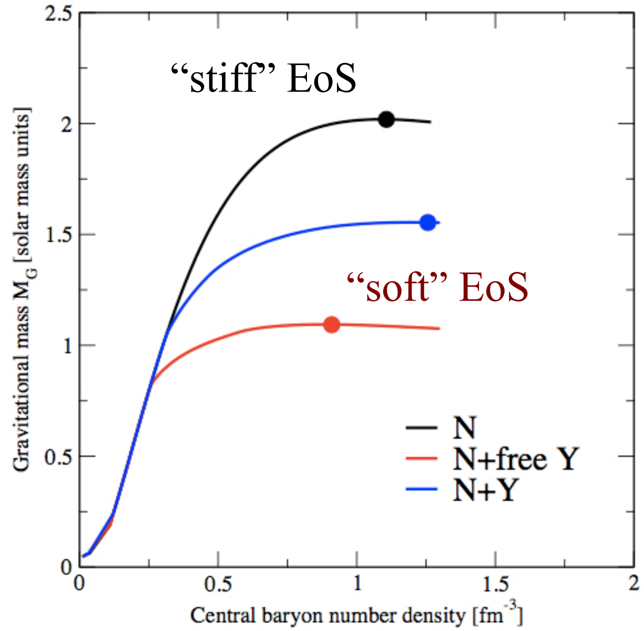

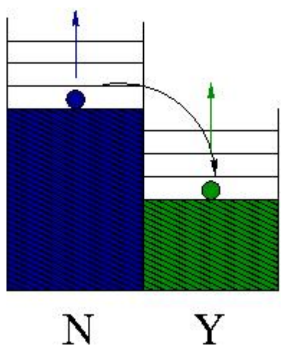

Relieve of Fermi pressure due to the appearance of hyperons ➔ EoS softer ➔ reduction of the mass

Measured Neutron Star Masses (up to ~ 2006-2008)

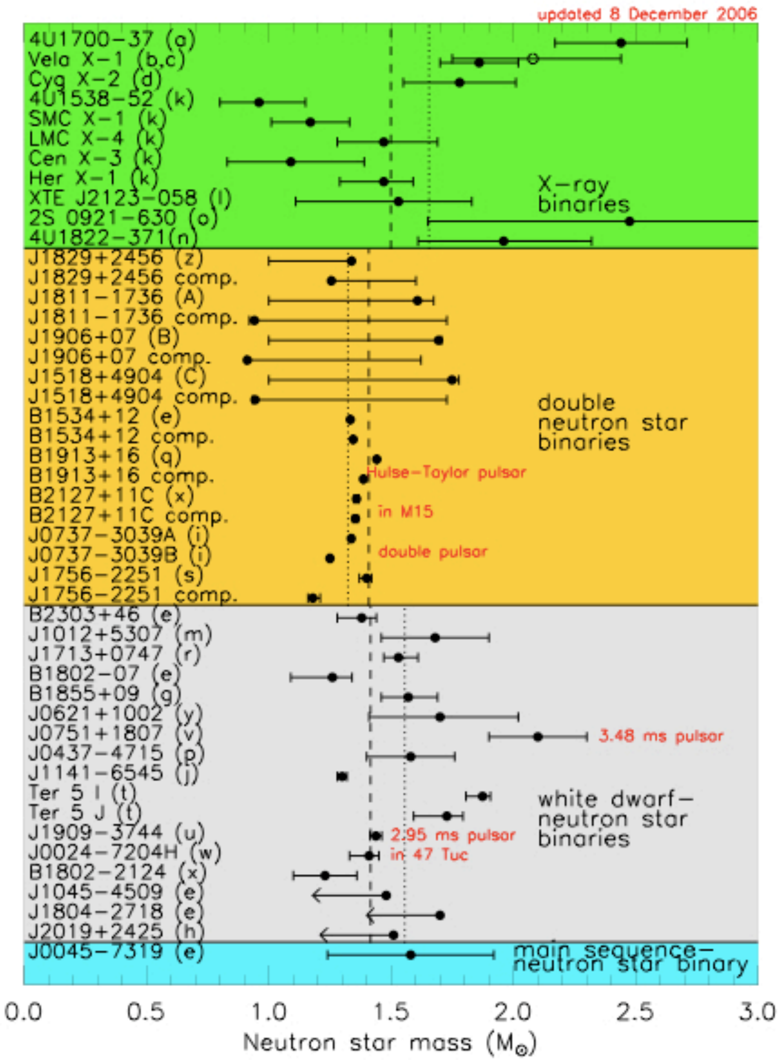

(Lattimer & Prakash 2007)

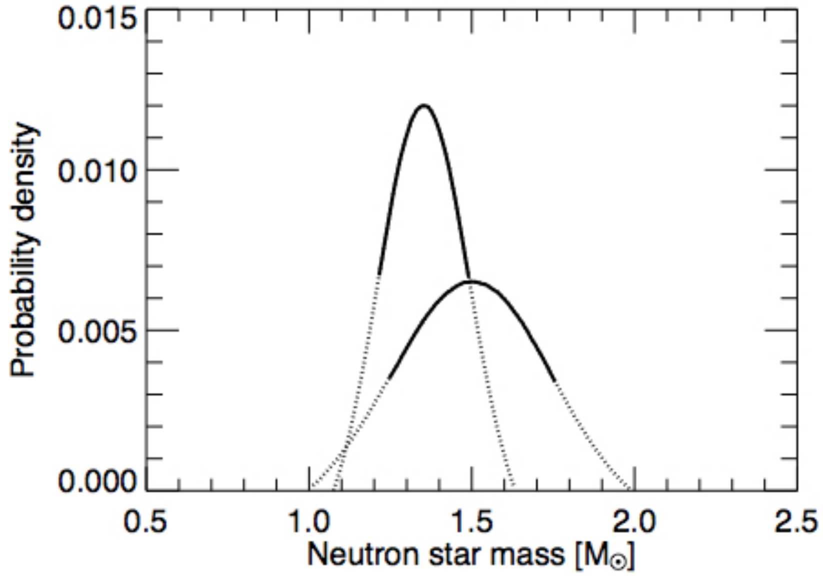

up to ~ 2006-2008 any valid EoS should predict

$$M_{\max}\left[EoS\right] > 1.4 - 1.5 M_{\odot}$$

Hyperons in NS
(up to ~ 2006-2008)

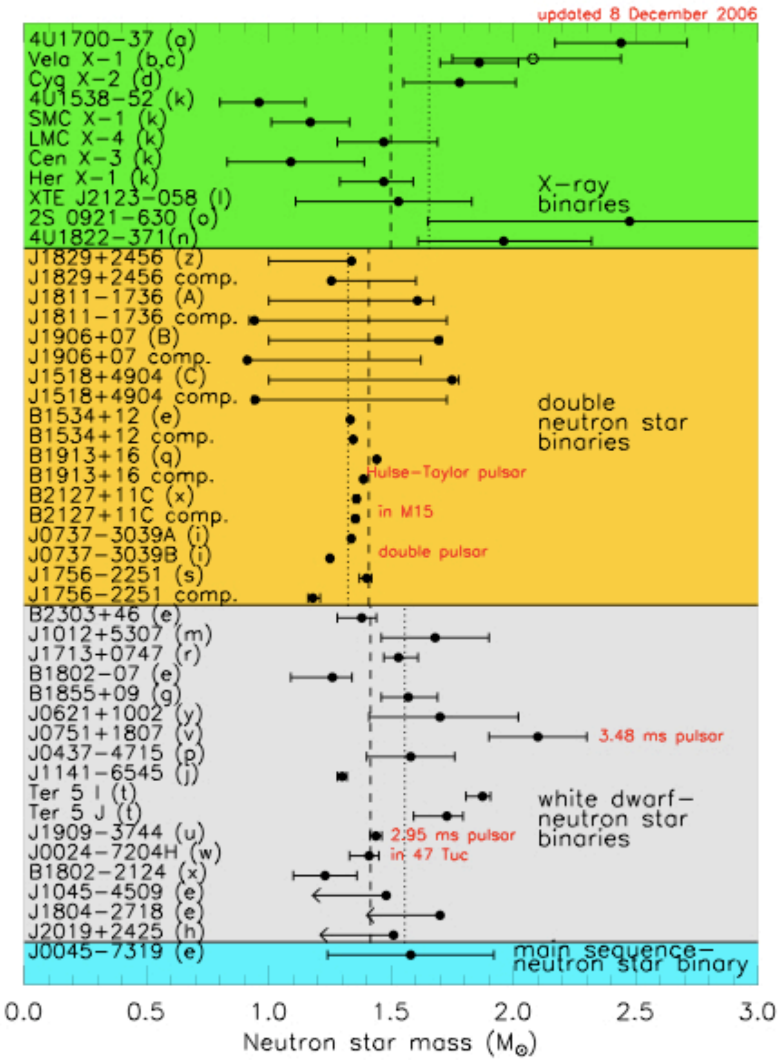

(Lattimer & Prakash 2007)

Phenomenological:
M_{max} compatible with 1.4-1.5 $M_\odot$

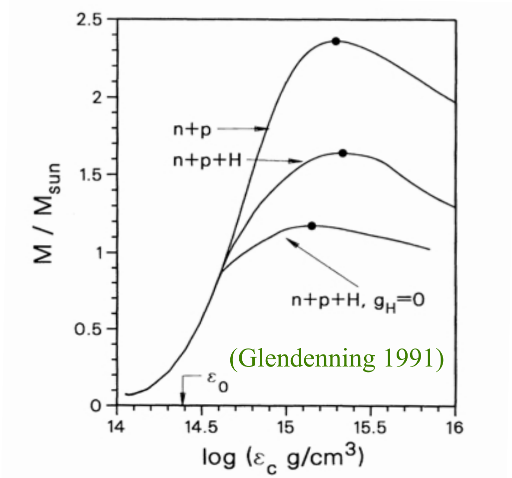

(Glendenning 1991)

Microscopic : M_{max} < 1.4-1.5 $M_\odot$

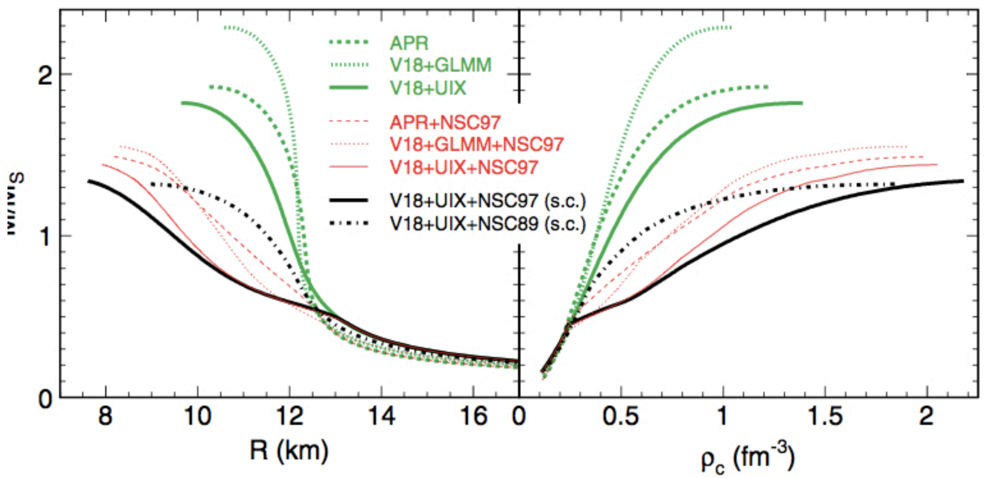

(Schulze, Polls, Ramos & IV 2006)

Recent measurements of high masses $\longrightarrow$ life of hyperons more difficult

Eccentric Binary Millisecond Pulsars

Paulo C. C. Freire

Arecibo Observatory, HC 3 Box 53995, Arecibo PR 00612, USA
West Virginia University, PO Box 6315, Morgantown WV 26505, USA

Abstract. In this paper we review recent discovery of millisecond pulsars (MSPs) in eccentric binary systems. Timing these MSPs we were able to estimate (and in one case precisely measure) their masses. These results suggest that, as a class, MSPs have a much wider range of masses (1.3 to $> 2M_{\odot}$) than the normal and mildly recycled pulsars found in double neutron star (DNS) systems ($1.25 < M_p < 1.44M_{\odot}$). This is very likely to be due to the prolonged accretion episode that is thought to be required to form a MSP. The likely existence of massive MSPs makes them a powerful probe for understanding the behavior of matter at densities larger than that of the atomic nucleus; in particular, the precise measurement of the mass of PSR J1903+0327 ($1.67 \pm 0.01M_{\odot}$) excludes several "soft" equations of state for dense matter.

Keywords: Neutron Stars, Pulsars, Binary Pulsars, General Relativity, Nuclear Equation of State
PACS: 97.60.Gb; 97.60.Jd; 97.80.Fk; 95.30.Sf; 26.60; 91.60.Fe

The precise measurement of the mass of PSR J1903+0328 (1.67 +/- 0.01 M_{sun}) excludes several "soft" EoS for dense matter

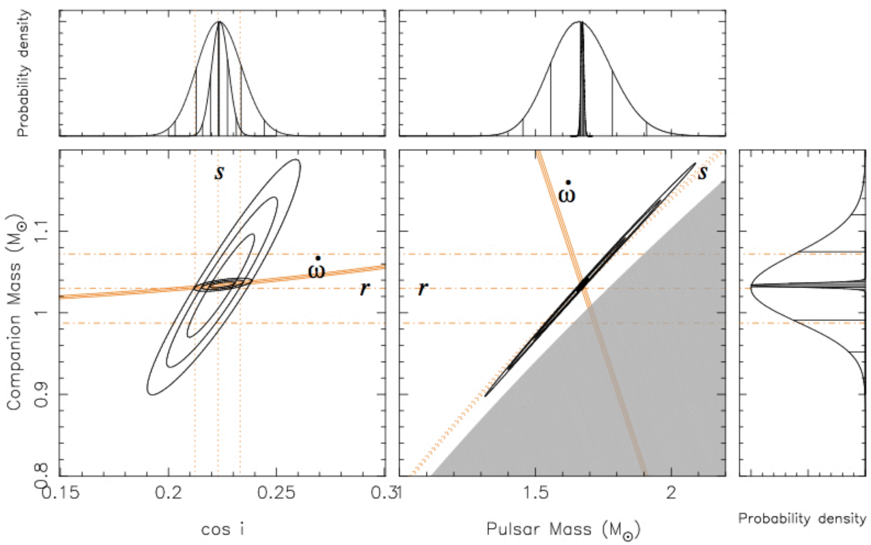

- ✓ binary sytem (P=95.17 d)
- ✓ high eccentricity (ε=0.437)
- ✓ companion mass: $\sim 1M_{\odot}$
- ✓ pulsar mass: $M = 1.67 \pm 0.11M_{\odot}$

Two-solar mass neutron star measured

Nature 464, 1081 (2010)

LETTER

doi:10.1038/nature09466

A two-solar-mass neutron star measured using Shapiro delay

P. B. Demorest[1], T. Pennucci[2], S. M. Ransom[1], M. S. E. Roberts[3] & J. W. T. Hessels[4,5]

Neutron stars are composed of the densest form of matter known to exist in our Universe, the composition and properties of which are still theoretically uncertain. Measurements of the masses or radii of these objects can strongly constrain the neutron star matter equation of state and rule out theoretical models of their composition[1,2]. The observed range of neutron star masses, however, has hitherto been too narrow to rule out many predictions of 'exotic' non-nucleonic components[3–6]. The Shapiro delay is a general-relativistic increase in light travel time through the curved space-time near a massive body[7]. For highly inclined (nearly edge-on) binary millisecond radio pulsar systems, this effect allows us to infer the masses of both the neutron star and its binary companion to high precision[8,9]. Here we present radio timing observations of the binary millisecond pulsar J1614-2230[10,11] that show a strong Shapiro delay signature. We calculate the pulsar mass to be $(1.97 \pm 0.04)M_\odot$, which rules out almost all currently proposed[2–5] hyperon or boson condensate equations of state ($M_\odot$, solar mass). Quark matter can support a star this massive only if the quarks are strongly interacting and are therefore not 'free' quarks[12].

long-term data set, parameter covariance and dispersion measure variation can be found in Supplementary Information.

As shown in Fig. 1, the Shapiro delay was detected in our data with extremely high significance, and must be included to model the arrival times of the radio pulses correctly. However, estimating parameter values and uncertainties can be difficult owing to the high covariance between many orbital timing model terms[14]. Furthermore, the χ^2 surfaces for the Shapiro-derived companion mass (M_2) and inclination angle (i) are often significantly curved or otherwise non-Gaussian[15]. To obtain robust error estimates, we used a Markov chain Monte Carlo (MCMC) approach to explore the post-fit χ^2 space and derive posterior probability distributions for all timing model parameters (Fig. 2). Our final results for the model

Table 1 | Physical parameters for PSR J1614-2230

Parameter	Value
Ecliptic longitude (λ)	245.78827556(5)°
Ecliptic latitude (β)	−1.256744(2)°
Proper motion in λ	9.79(7) mas yr^{-1}
Proper motion in β	−30(3) mas yr^{-1}
Parallax	0.5(6) mas

The mass 1.97 +/- 0.04 M_{sun} of the pulsar PSR J1614+2230 rules out almost all currently proposed hyperon or boson condensate EoS. Quark matter can support such a massive star only if quarks are strongly interacting (not "free quarks")

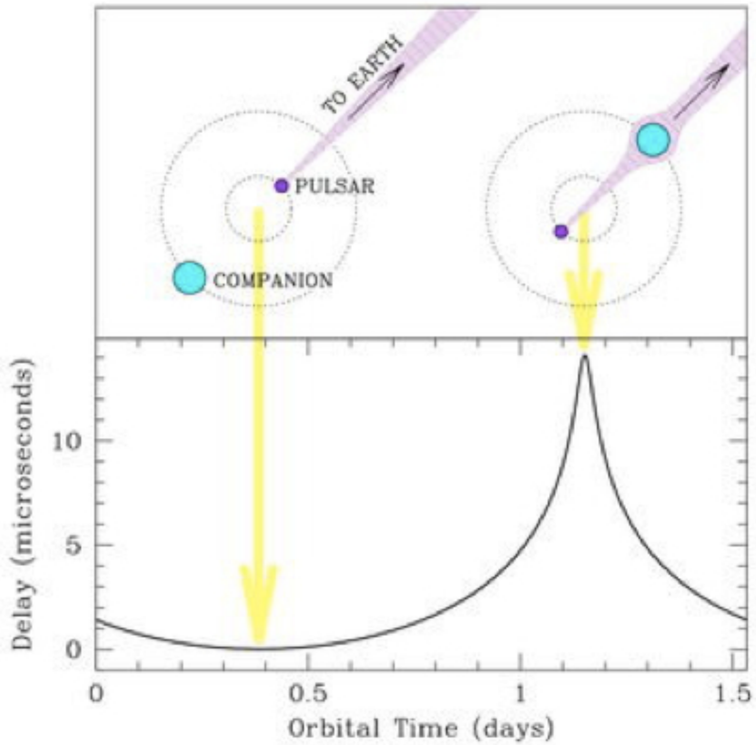

Binary millisecond pulsar PSR J1614+2230
Shapiro delay signature

$$\Delta t = -\frac{2GM}{c^3}\log\left(1 - \vec{R}\cdot\vec{R}'\right)$$

On April 26th 2013 the discovery of the most massive (up to now) pulsar (PSR J0348+0432) was made public

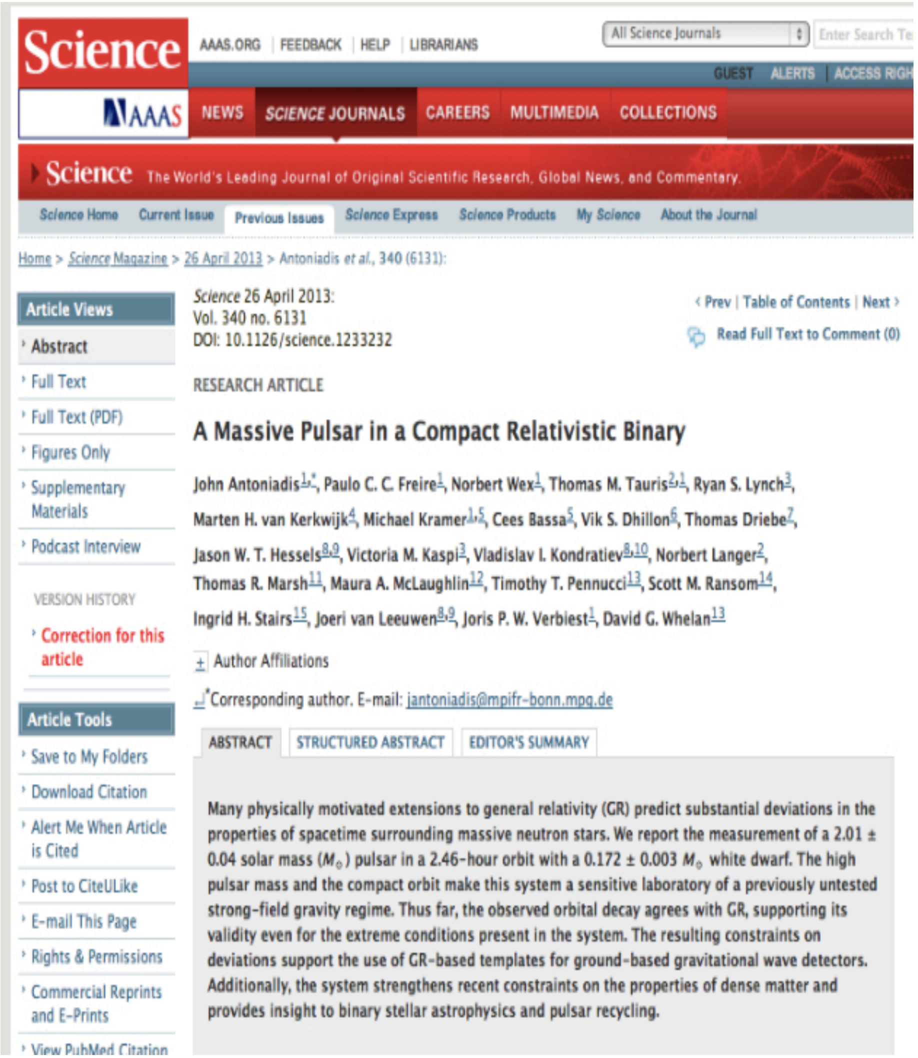
Science | AAAS.ORG | FEEDBACK | HELP | LIBRARIANS

NEWS | SCIENCE JOURNALS | CAREERS | MULTIMEDIA | COLLECTIONS

Science The World's Leading Journal of Original Scientific Research, Global News, and Commentary.

Science Home | Current Issue | Previous Issues | Science Express | Science Products | My Science | About the Journal

Home > Science Magazine > 26 April 2013 > Antoniadis et al., 340 (6131):

Science 26 April 2013:
Vol. 340 no. 6131
DOI: 10.1126/science.1233232

RESEARCH ARTICLE

A Massive Pulsar in a Compact Relativistic Binary

John Antoniadis[1,*], Paulo C. C. Freire[1], Norbert Wex[1], Thomas M. Tauris[2,1], Ryan S. Lynch[3], Marten H. van Kerkwijk[4], Michael Kramer[1,5], Cees Bassa[5], Vik S. Dhillon[6], Thomas Driebe[7], Jason W. T. Hessels[8,9], Victoria M. Kaspi[3], Vladislav I. Kondratiev[8,10], Norbert Langer[2], Thomas R. Marsh[11], Maura A. McLaughlin[12], Timothy T. Pennucci[13], Scott M. Ransom[14], Ingrid H. Stairs[15], Joeri van Leeuwen[8,9], Joris P. W. Verbiest[1], David G. Whelan[13]

Author Affiliations

*Corresponding author. E-mail: jantoniadis@mpifr-bonn.mpg.de

ABSTRACT | STRUCTURED ABSTRACT | EDITOR'S SUMMARY

Many physically motivated extensions to general relativity (GR) predict substantial deviations in the properties of spacetime surrounding massive neutron stars. We report the measurement of a 2.01 ± 0.04 solar mass ($M_\odot$) pulsar in a 2.46-hour orbit with a 0.172 ± 0.003 $M_\odot$ white dwarf. The high pulsar mass and the compact orbit make this system a sensitive laboratory of a previously untested strong-field gravity regime. Thus far, the observed orbital decay agrees with GR, supporting its validity even for the extreme conditions present in the system. The resulting constraints on deviations support the use of GR-based templates for ground-based gravitational wave detectors. Additionally, the system strengthens recent constraints on the properties of dense matter and provides insight to binary stellar astrophysics and pulsar recycling.

Article Views: Abstract, Full Text, Full Text (PDF), Figures Only, Supplementary Materials, Podcast Interview

VERSION HISTORY: Correction for this article

Article Tools: Save to My Folders, Download Citation, Alert Me When Article is Cited, Post to CiteULike, E-mail This Page, Rights & Permissions, Commercial Reprints and E-Prints, View PubMed Citation

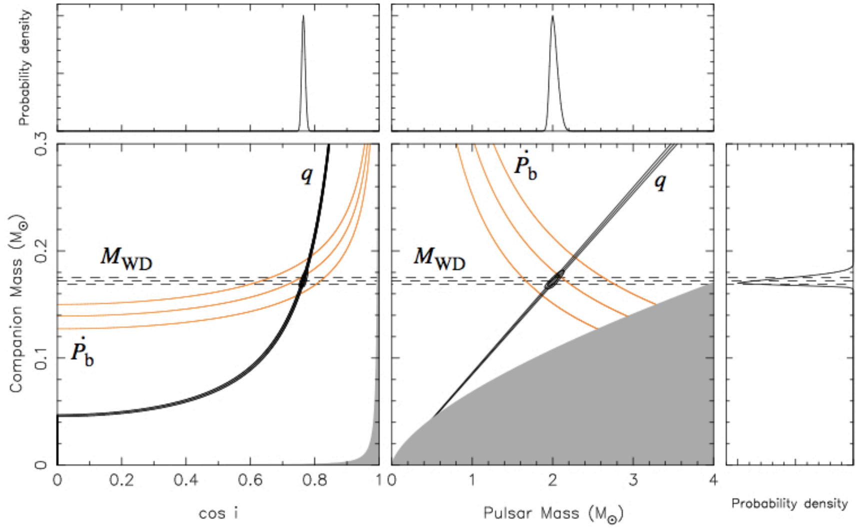

- ✓ binary system (P=2.46 h)
- ✓ very low eccentricity
- ✓ companion mass: $0.172 \pm 0.003 M_\odot$
- ✓ pulsar mass: $M = 2.01 \pm 0.04 M_\odot$

Measured Neutron Star Masses (2014)

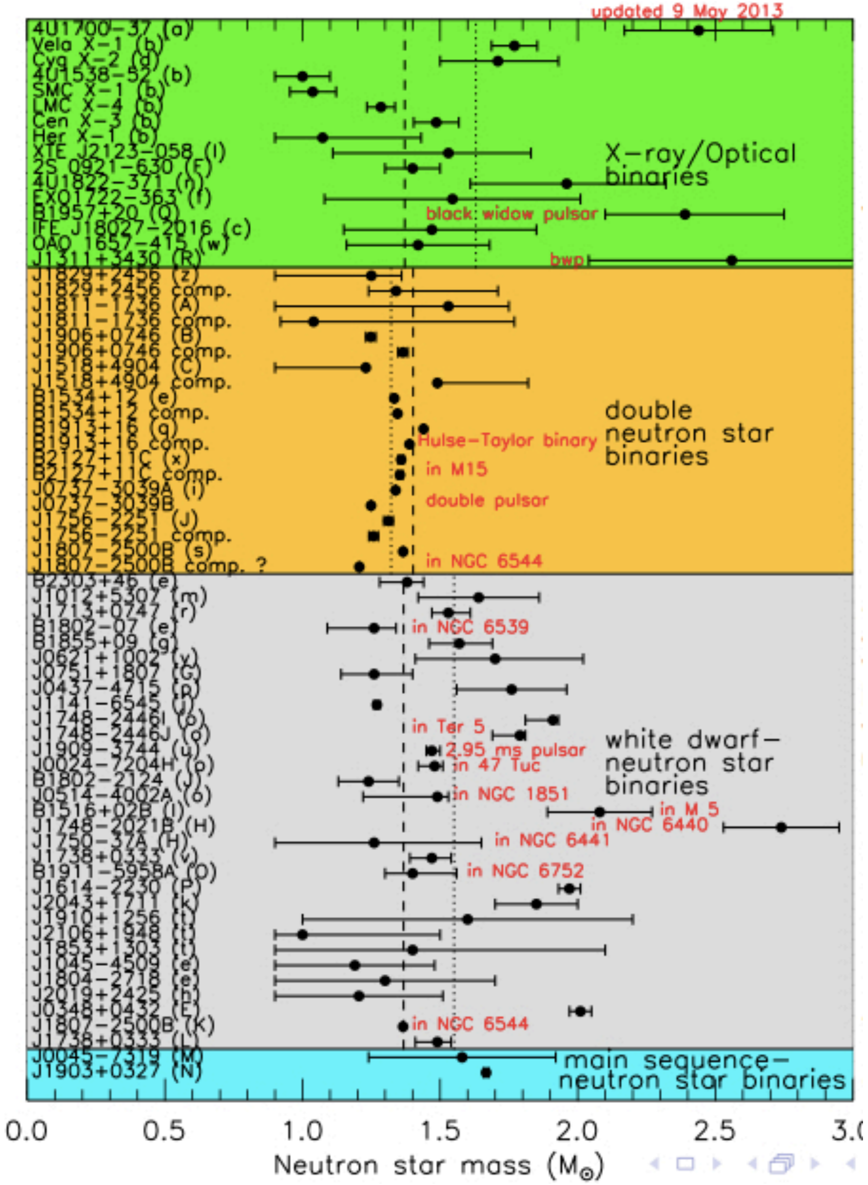

updated from Lattimer 2013

Observation of ~ 2 M_{sun} neutron stars

↓

Dense matter EoS stiff enough is required such that

$$M_{\max}\left[EoS\right] > 2M_\odot$$

Can hyperons still be present in the interior of neutron stars in view of this constraint ?

The Hyperon Puzzle

"Hyperons → "soft (or too soft) EoS" not compatible (mainly in microscopic approaches) with measured (high) masses. However, the presence of hyperons in the NS interior seems to be unavoidable."

- ✓ can YN & YY interactions still solve it ?
- ✓ or perhaps hyperonic three-body forces ?
- ✓ what about quark matter ?

Can Hyperonic TBF solve this puzzle ?

Natural solution based on: Importance of NNN force in Nuclear Physics

(Considered by several authors: Chalk, Gal, Usmani, Bodmer, Takatsuka, Loiseau, Nogami, Bahaduri, IV)

<u>NNN Force</u>

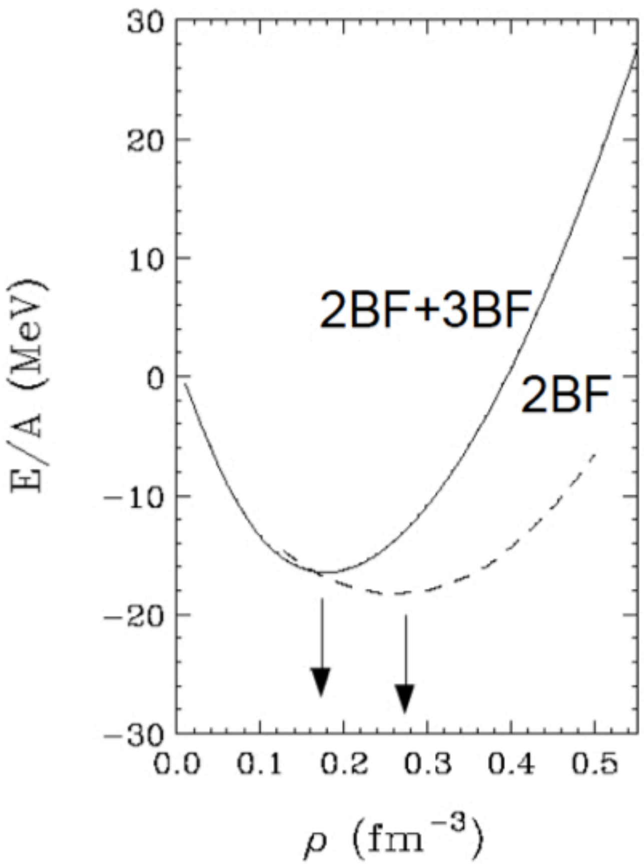

<u>NNY, NYY & YYY Forces</u>

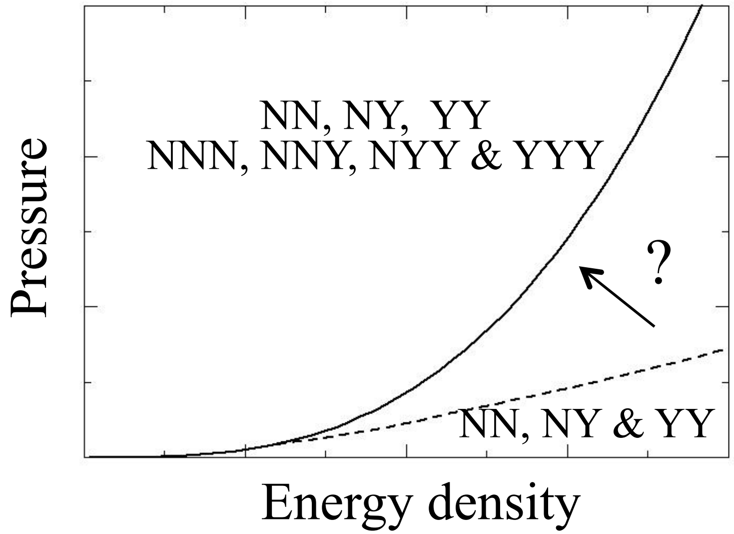

Can hyperonic TBF provide enough repulsion at high densities to reach $2M_\odot$?

Two-meson exchange Hyperonic TBF

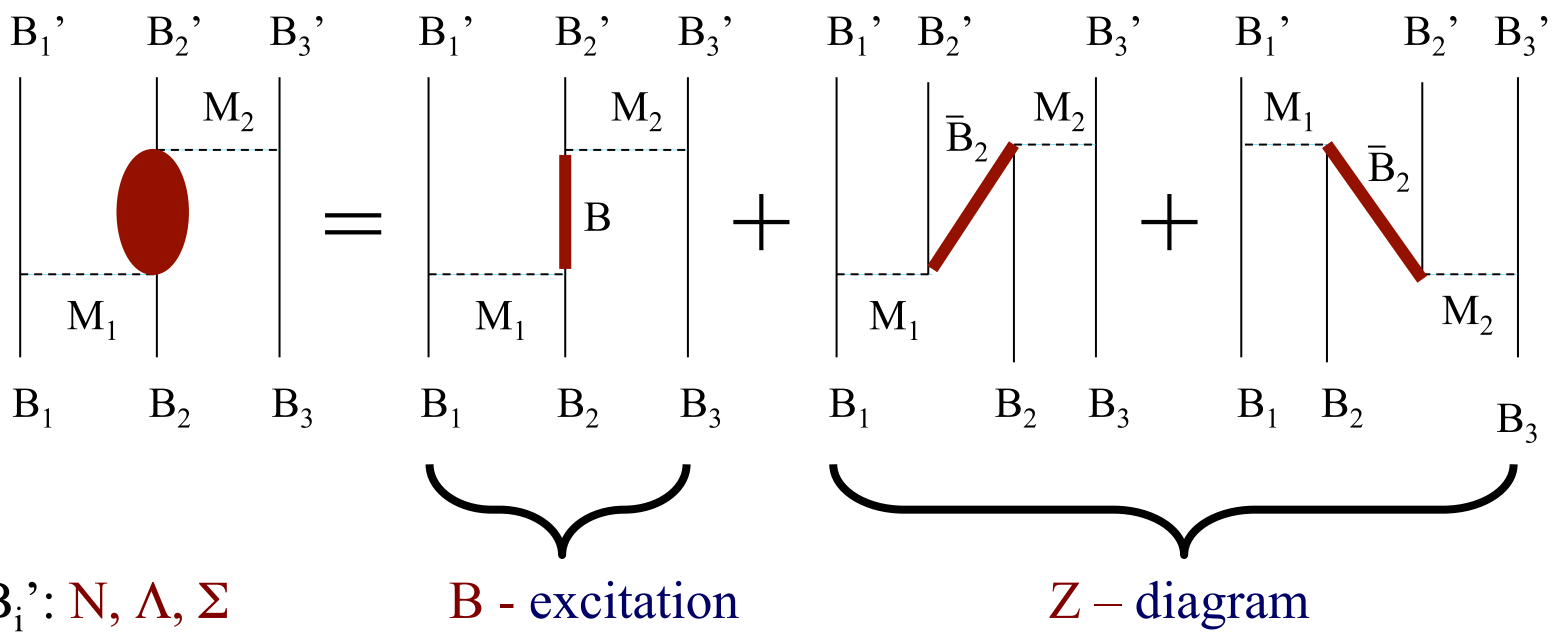

B_i B_i': N, Λ, Σ

M_i: π, K, σ, ω

B: Λ, Σ, Δ, Σ*

$\bar{B}_2$: $\bar{N}$, $\bar{\Lambda}$, $\bar{\Sigma}$

Vertices: consistent with YN and YY

Repulsion at high densities due to Z-diagram as in NNN

Baryon-excitation contribution
(π-, *K*-exchange)

$$V_{NNY}^{M_1M_2,B} = C_{NNY}^{M_1M_2,B}\left(\hat{O}_A\left\{X_{12}(\vec{r}_{12}),X_{23}(\vec{r}_{23})\right\}\right.$$
$$\left.+\hat{O}_B\left[X_{12}(\vec{r}_{12}),X_{23}(\vec{r}_{23})\right]\right)$$

$\hat{O}_A,\hat{O}_B \rightarrow$ isospin structure

$$X_{ij}(\vec{x}) = \vec{\sigma}_i\cdot\vec{\sigma}_j Y_{ij}(x) + \hat{S}_{ij}(\hat{x})T_{ij}(x)$$

$$Y_{ij}(x) = \frac{\partial^2 Z_{ij}}{\partial x^2} + \frac{2}{x}\frac{\partial Z_{ij}}{\partial x},\quad T_{ij}(x) = \frac{\partial^2 Z_{ij}}{\partial x^2} - \frac{1}{x}\frac{\partial Z_{ij}}{\partial x}$$

$$Z_{12}(x) = \frac{4\pi}{m_{M_1}}\int\frac{d\vec{k}}{(2\pi)^3}\frac{e^{-i\vec{k}\cdot\vec{x}}}{k^2+m_{M_1}^2}F_{B_1B_1^{'}M_1}(k^2)F_{B_2BM_1}(k^2)$$

$$Z_{23}(x) = \frac{4\pi}{m_{M_2}}\int\frac{d\vec{q}}{(2\pi)^3}\frac{e^{-i\vec{q}\cdot\vec{x}}}{q^2+m_{M_2}^2}F_{B_3B_3^{'}M_2}(q^2)F_{B_2^{'}BM_2}(q^2)$$

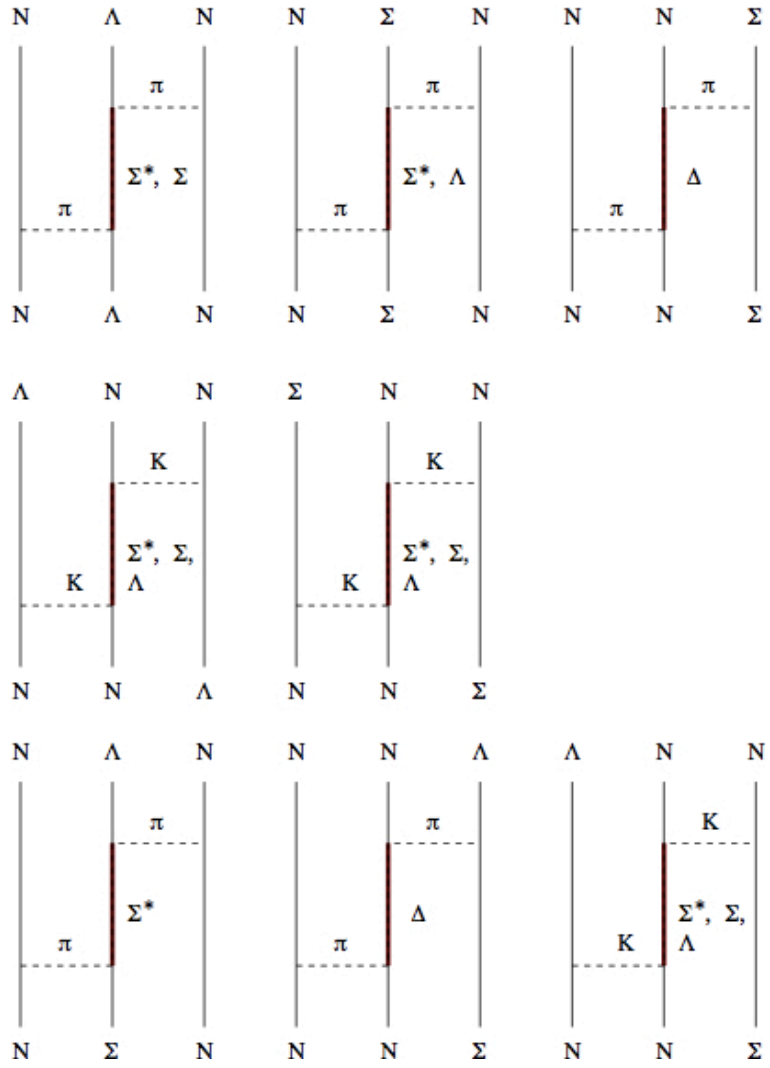

Isospin structure: operators $\hat{O}_{\mathrm{A}}$ & $\hat{O}_{\mathrm{B}}$

$$V_{NNY}^{M_1M_2,B} = C_{NNY}^{M_1M_2,B}\left(\hat{O}_A\left\{X_{12}(\vec{r}_{12}),X_{23}(\vec{r}_{23})\right\}+\hat{O}_A\left[X_{12}(\vec{r}_{12}),X_{23}(\vec{r}_{23})\right]\right)$$

$V_{NNY}^{M_1M_2,B}$	$\hat{O}_A$	$\hat{O}_B$
$V_{NN\Lambda}^{\pi\pi,\Sigma^*}, V_{NN\Lambda}^{\pi\pi,\Sigma}, V_{NN\Sigma}^{\pi\pi,\Sigma^*}, V_{NN\Sigma}^{\pi\pi,\Lambda}, V_{NN\Sigma}^{KK,\Lambda}, V_{NN\Sigma\leftrightarrow NN\Lambda}^{\pi\pi,\Sigma^*}$	$\vec{\tau}_1\cdot\vec{\tau}_3$	—
$V_{NN\Sigma}^{\pi\pi,\Delta}$	$\left\{\vec{\tau}_1\cdot\vec{\tau}_2,\vec{\tau}_2\cdot\vec{I}_3\right\}$	$\frac{1}{4}\left[\vec{\tau}_1\cdot\vec{\tau}_2,\vec{\tau}_2\cdot\vec{I}_3\right]$
$V_{NN\Sigma\leftrightarrow NN\Lambda}^{\pi\pi,\Delta}$	$\left\{\vec{\tau}_1\cdot\vec{\tau}_2,\vec{\tau}_2\cdot\vec{\rho}_3\right\}$	$\frac{1}{4}\left[\vec{\tau}_1\cdot\vec{\tau}_2,\vec{\tau}_2\cdot\vec{\rho}_3\right]$
$V_{NN\Lambda}^{KK,\Sigma^*}$	$\left\{\vec{1}_1\cdot\vec{\tau}_2,\vec{\tau}_2\cdot\vec{1}_3\right\}$	$-\frac{1}{2}\left[\vec{1}_1\cdot\vec{\tau}_2,\vec{\tau}_2\cdot\vec{1}_3\right]$
$V_{NN\Lambda}^{KK,\Sigma}$	$\left\{\vec{1}_1\cdot\vec{\tau}_2,\vec{\tau}_2\cdot\vec{1}_3\right\}$	$\left[\vec{1}_1\cdot\vec{\tau}_2,\vec{\tau}_2\cdot\vec{1}_3\right]$
$V_{NN\Lambda}^{KK,\Lambda}$	1	—

Isospin structure: operators $\hat{O}_A$ & $\hat{O}_B$ (cont')

$$V_{NNY}^{M_1M_2,B} = C_{NNY}^{M_1M_2,B}\left(\hat{O}_A\left\{X_{12}(\vec{r}_{12}),X_{23}(\vec{r}_{23})\right\}+\hat{O}_A\left[X_{12}(\vec{r}_{12}),X_{23}(\vec{r}_{23})\right]\right)$$

$V_{NNY}^{M_1M_2,B}$	$\hat{O}_A$	$\hat{O}_B$
$V_{NN\Sigma}^{KK,\Sigma^*}$	$\left\{\vec{\tau}_1\cdot\vec{\tau}_2,\vec{\tau}_2\cdot\vec{\tau}_3\right\}$	$-\frac{1}{2}\left[\vec{\tau}_1\cdot\vec{\tau}_2,\vec{\tau}_2\cdot\vec{\tau}_3\right]$
$V_{NN\Sigma}^{KK,\Sigma}$	$\left\{\vec{\tau}_1\cdot\vec{\tau}_2,\vec{\tau}_2\cdot\vec{\tau}_3\right\}$	$\left[\vec{\tau}_1\cdot\vec{\tau}_2,\vec{\tau}_2\cdot\vec{\tau}_3\right]$
$V_{NN\Sigma\leftrightarrow NN\Lambda}^{KK,\Sigma^*}$	$\left\{\vec{\rho}_1\cdot\vec{\tau}_2,\vec{\tau}_2\cdot\vec{\tau}_3\right\}$	$-\frac{1}{2}\left[\vec{\rho}_1\cdot\vec{\tau}_2,\vec{\tau}_2\cdot\vec{\tau}_3\right]$
$V_{NN\Sigma\leftrightarrow NN\Lambda}^{KK,\Sigma}$	$\left\{\vec{\rho}_1\cdot\vec{\tau}_2,\vec{\tau}_2\cdot\vec{\tau}_3\right\}$	$\left[\vec{\rho}_1\cdot\vec{\tau}_2,\vec{\tau}_2\cdot\vec{\tau}_3\right]$
$V_{NN\Sigma\leftrightarrow NN\Lambda}^{KK,\Lambda}$	$\vec{\rho}_1\cdot\vec{\tau}_2$	—

Z-diagram contribution (σ,ω-exchange)

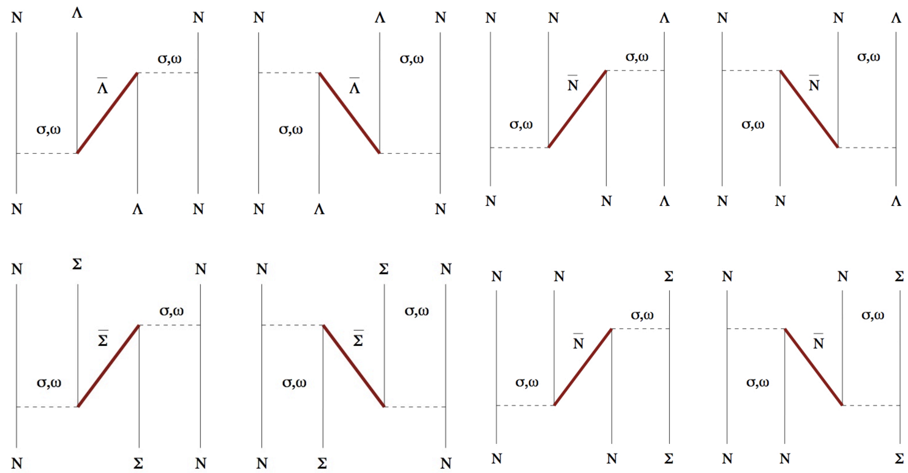

- <u>σσ–exchange contribution</u>

$$V_{NNY}^{\sigma\sigma,\bar{B}} = C_{NNY}^{\sigma\sigma,\bar{B}}\Big(-4Z_{12}(r_{12})Z_{23}(r_{23})\nabla^2_{r_2'} - 4Z_{12}'(r_{12})Z_{23}(r_{23})\hat{r}_{12}\cdot\nabla_{r_2'}$$

$$-4Z_{12}(r_{12})Z_{23}'(r_{23})\hat{r}_{23}\cdot\nabla_{r_2'} - \big(Y_{12}(r_{12})Z_{23}(r_{23}) + Z_{12}(r_{12})Y_{23}(r_{23})\big)$$

$$-\hat{r}_{12}\cdot\hat{r}_{23}Z_{12}'(r_{12})Z_{23}'(r_{23}) - 2i\Big(Z_{12}'(r_{12})Z_{23}(r_{23})\vec{\sigma}_2\cdot\hat{r}_{12}\times\nabla_{r_2'}$$

$$+Z_{12}(r_{12})Z_{23}'(r_{23})\vec{\sigma}_2\cdot\hat{r}_{23}\times\nabla_{r_2'}\Big)\Big)\delta\left(\vec{r}_1-\vec{r}_1^{\,'}\right)\delta\left(\vec{r}_2-\vec{r}_2^{\,'}\right)\delta\left(\vec{r}_3-\vec{r}_3^{\,'}\right)$$

- ωω–exchange contribution

$$V_{NNY}^{\omega\omega,\bar{B}} = C_{NNY}^{\omega\omega,\bar{B}} \Big(\Big(\big(1+\vec{\sigma}_1\cdot\vec{\sigma}_2+\vec{\sigma}_1\cdot\vec{\sigma}_2+\vec{\sigma}_2\cdot\vec{\sigma}_3\big)\hat{r}_{12}\cdot\hat{r}_{23}-\vec{\sigma}_1\cdot\hat{r}_{23}\vec{\sigma}_2\cdot\hat{r}_{12}-\vec{\sigma}_2\cdot\hat{r}_{23}\vec{\sigma}_3\cdot\hat{r}_{12}$$

$$-\vec{\sigma}_1\cdot\hat{r}_{23}\vec{\sigma}_3\cdot\hat{r}_{12}\Big)Z_{12}^{'}(r_{12})Z_{23}^{'}(r_{23})-2iZ_{12}^{'}(r_{12})Z_{23}(r_{23})\big(\vec{\sigma}_2+\vec{\sigma}_3\big)\cdot\hat{r}_{12}\times\nabla_{r_3^{'}}$$

$$-2iZ_{12}(r_{12})Z_{23}^{'}(r_{23})\big(\vec{\sigma}_2+\vec{\sigma}_3\big)\cdot\hat{r}_{23}\times\nabla_{r_2^{'}}-4Z_{12}(r_{12})Z_{23}(r_{23})\nabla_{r_1^{'}}\cdot\nabla_{r_3^{'}}\Big)$$

$$\delta\big(\vec{r}_1-\vec{r}_1^{\,'}\big)\delta\big(\vec{r}_2-\vec{r}_2^{\,'}\big)\delta\big(\vec{r}_3-\vec{r}_3^{\,'}\big)$$

- σω–exchange contribution

$$V_{NNY}^{\sigma\omega,\bar{B}} = C_{NNY}^{\sigma\omega,\bar{B}} \Big(\Big(\big(1+\vec{\sigma}_2\cdot\vec{\sigma}_3\big)Z_{12}(r_{12})Y_{23}(r_{23})-2iZ_{12}(r_{12})Z_{23}^{'}(r_{23})\big(\vec{\sigma}_2+\vec{\sigma}_3\big)\cdot\hat{r}_{23}\times\nabla_{r_2^{'}}$$

$$+2iZ_{12}^{'}(r_{12})Z_{23}^{'}(r_{23})\big(\vec{\sigma}_2+\vec{\sigma}_3\big)\cdot\hat{r}_{12}\times\hat{r}_{23}+2iZ_{12}(r_{12})Z_{23}^{'}(r_{23})\vec{\sigma}_2\cdot\hat{r}_{23}\times\nabla_{r_3^{'}}$$

$$+2Z_{12}^{'}(r_{12})Z_{23}(r_{23})\hat{r}_{12}\cdot\nabla_{r_3^{'}}+2Z_{12}(r_{12})Z_{23}^{'}(r_{23})\hat{r}_{23}\cdot\nabla_{r_3^{'}}+4Z_{12}(r_{12})Z_{23}(r_{23})\nabla_{r_2^{'}}\cdot\nabla_{r_3^{'}}$$

$$-\frac{1}{3}\Big(\vec{\sigma}_2\cdot\vec{\sigma}_3Y_{12}(r_{12})+\hat{S}_{23}(\hat{r}_{23})T_{23}(r_{23})\Big)Z_{12}(r_{12})\Big)$$

$$+D_{NNY}^{\sigma\omega,\bar{B}}\Big(-Y_{12}(r_{12})+Y_{23}(r_{23})-4Z_{12}^{'}(r_{12})Z_{23}^{'}(r_{23})-3Z_{12}^{'}(r_{12})\nabla_{r_2^{'}}\cdot\hat{r}_{12}\Big)$$

$$+i\vec{\sigma}_2\cdot\Big(2\nabla_{r_{23}}\times\nabla_{r_{12}}-5\nabla_{r_2^{'}}\times\hat{r}_{23}\Big)Z_{12}(r_{12})Z_{23}(r_{23})$$

$$+\Big(\vec{r}_{12}\leftrightarrow\vec{r}_{23},\vec{r}_1\leftrightarrow\vec{r}_1^{\,'},\vec{r}_2\leftrightarrow\vec{r}_2^{\,'},\vec{\sigma}_1\leftrightarrow\vec{\sigma}_3\Big)\Big)\delta(\vec{r}_1-\vec{r}_1^{\,'})\delta(\vec{r}_2-\vec{r}_2^{\,'})\delta(\vec{r}_3-\vec{r}_3^{\,'})$$

But that's only the beginning of the full story

there are

MANY, MANY, MANY more forces & contributions ....

BHF approximation of Hyperonic Matter

Energy per particle

- $$\frac{E}{A}(\rho,\beta)=\frac{1}{A}\sum_{B}\sum_{k\le k_{F_B}}\left(\frac{\hbar^2k^2}{2m_B}+\frac{1}{2}\mathrm{Re}\left[U_B(\vec{k})\right]\right)$$

Infinite sumation of two-hole line diagrams

Bethe-Goldstone Equation

- $$G(\omega)=V+V\frac{Q}{\omega-E-E'+i\eta}G(\omega)$$
- $$E_B(k)=\frac{\hbar^2k^2}{2m_B}+\mathrm{Re}\left[U_N(k)\right]+m_B$$
- $$U_B(k)=\sum_{B'}\sum_{k'\le k_{F_{B'}}}\left\langle \vec{k}\vec{k}'\middle|G\left(\omega=E_B(k)+E_{B'}(k')\right)\middle|\vec{k}\vec{k}'\right\rangle$$

Partial sumation of pp ladder diagrams

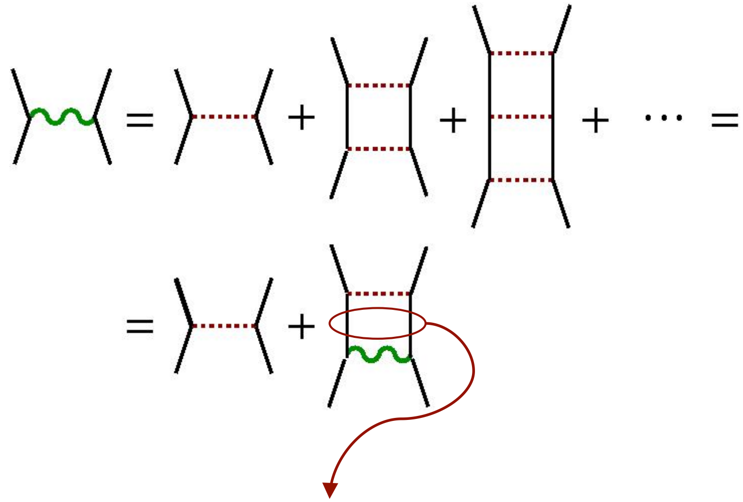

- ✓ Pauli blocking
- ✓ Baryon dressing

Three-Body Forces within the BHF approach

TBF can be introduced in our BHF approach by adding effective density-dependent two body forces to the baryon-baryon interactions V when solving the Bethe-Goldstone equation

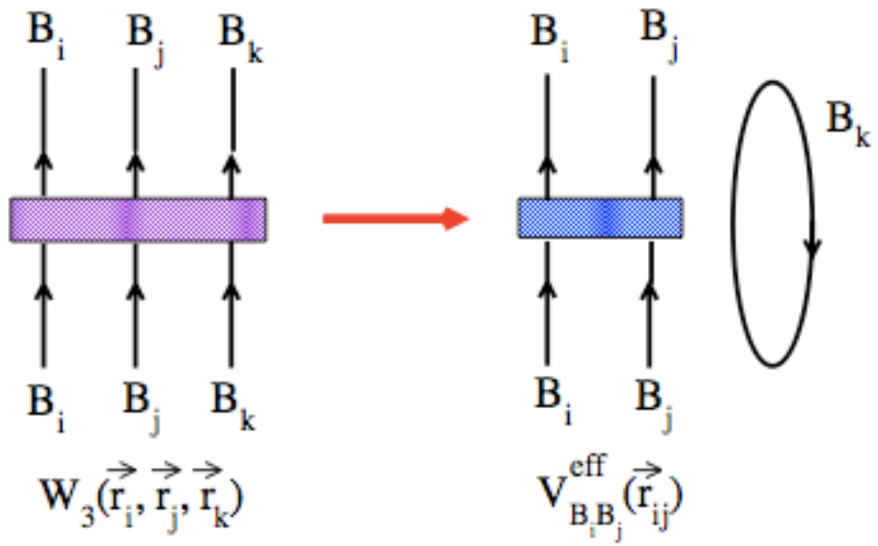

$$V_{B_iB_j}^{eff}\left(\vec{r}_{ij}\right)=\int W_3\left(\vec{r}_i,\vec{r}_j,\vec{r}_k\right)n\left(\vec{r}_i,\vec{r}_j,\vec{r}_k\right)d^3\vec{r}_k$$

$W_3\left(\vec{r}_i,\vec{r}_j,\vec{r}_k\right)$: genuine TBF

$n\left(\vec{r}_i,\vec{r}_j,\vec{r}_k\right)$: three-body correlation function

From the genuine NNN,NNY, NYY and YYY TBF …

NNN ➔ NN

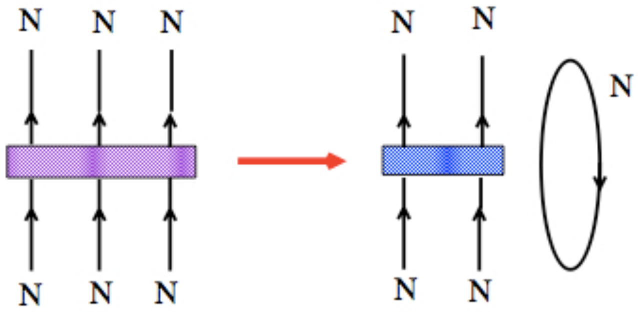

NNY ➔ NN, NY

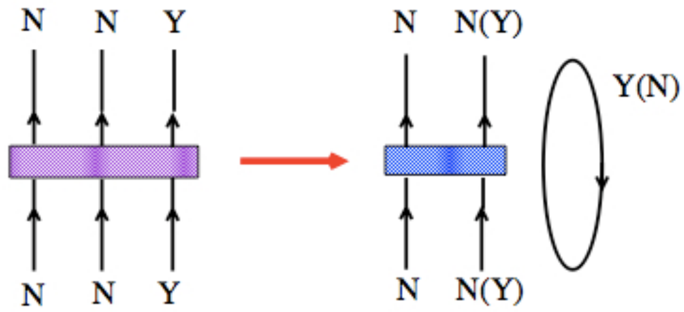

NYY ➔ NY, YY

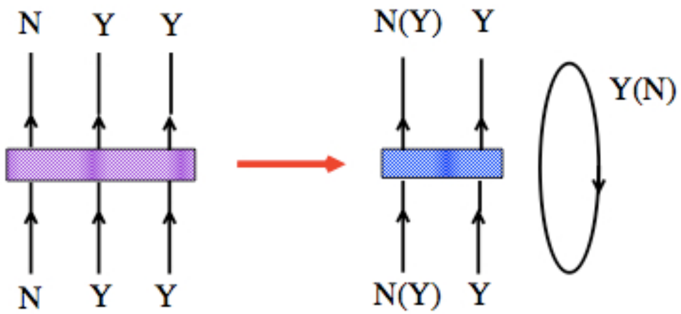

YYY ➔ YY

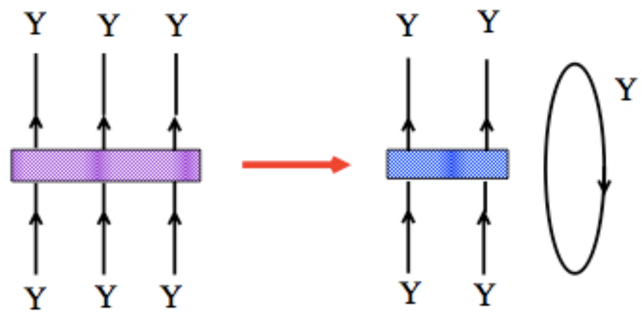

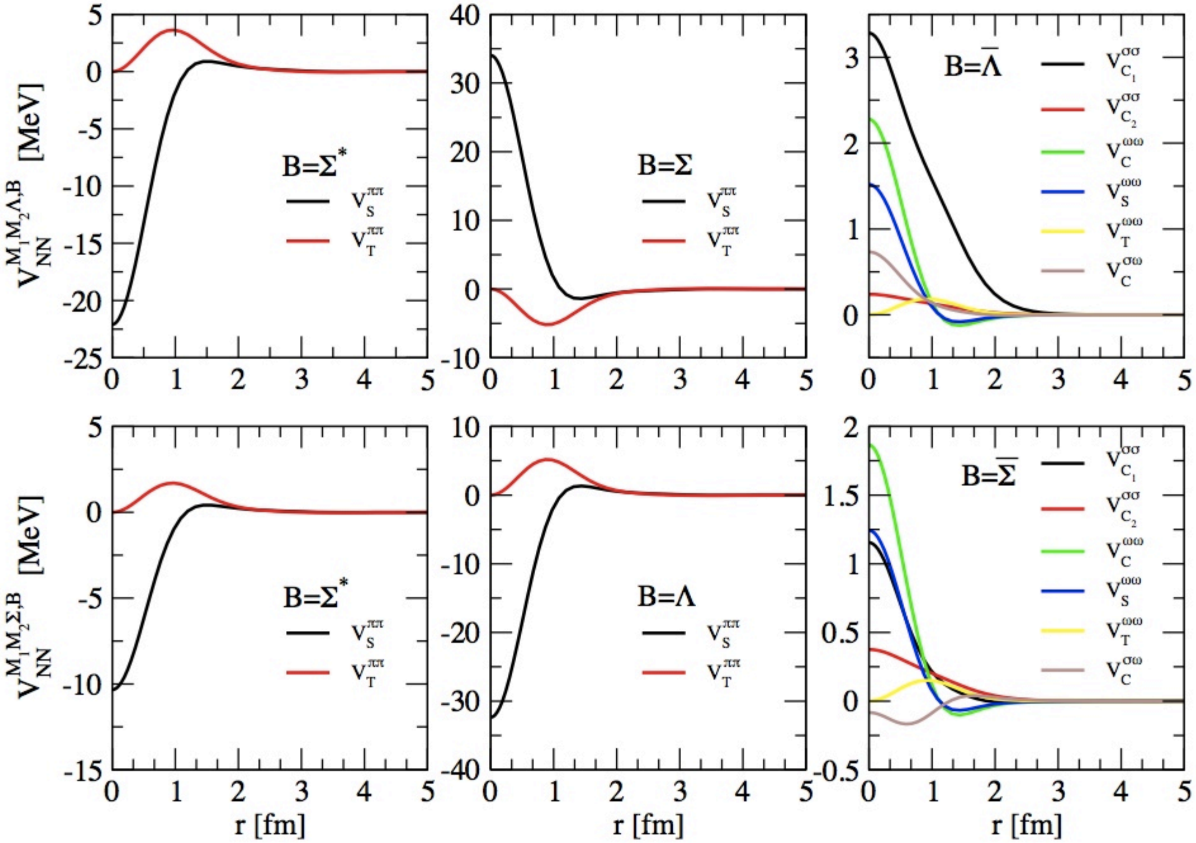

Effective NN density-dependent 2BF from NNY

- $V_{NN}^{\pi\pi Y,B}\left(\vec{r}\right)=C_{NNY}^{\pi\pi,B}\rho_Y\left[V_S^{\pi\pi}\left(\vec{r}\right)\vec{\sigma}_1\cdot\vec{\sigma}_2+V_T^{\pi\pi}\left(\vec{r}\right)S_{12}\left(\hat{r}\right)\right]\vec{\tau}_1\cdot\vec{\tau}_2$
- $V_{NN}^{\sigma\sigma Y,\bar{B}}\left(\vec{r}\right)=C_{NNY}^{\sigma\sigma,\bar{B}}\left[\rho_N V_{C_1}^{\sigma\sigma}\left(\vec{r}\right)+\rho_N^{5/3}V_{C_2}^{\sigma\sigma}\left(\vec{r}\right)\right]$
- $V_{NN}^{\omega\omega Y,\bar{B}}\left(\vec{r}\right)=C_{NNY}^{\omega\omega,\bar{B}}\rho_Y\left[V_C^{\omega\omega}\left(\vec{r}\right)+V_S^{\omega\omega}\left(\vec{r}\right)\vec{\sigma}_1\cdot\vec{\sigma}_2+V_T^{\omega\omega}\left(\vec{r}\right)S_{12}\left(\hat{r}\right)\right]$
- $V_{NN}^{\sigma\omega Y,\bar{B}}\left(\vec{r}\right)=C_{NNY}^{\sigma\omega,\bar{B}}\rho_N V_C^{\sigma\omega}\left(\vec{r}\right)$

Effective NΛ density-dependent 2BF from NNΛ

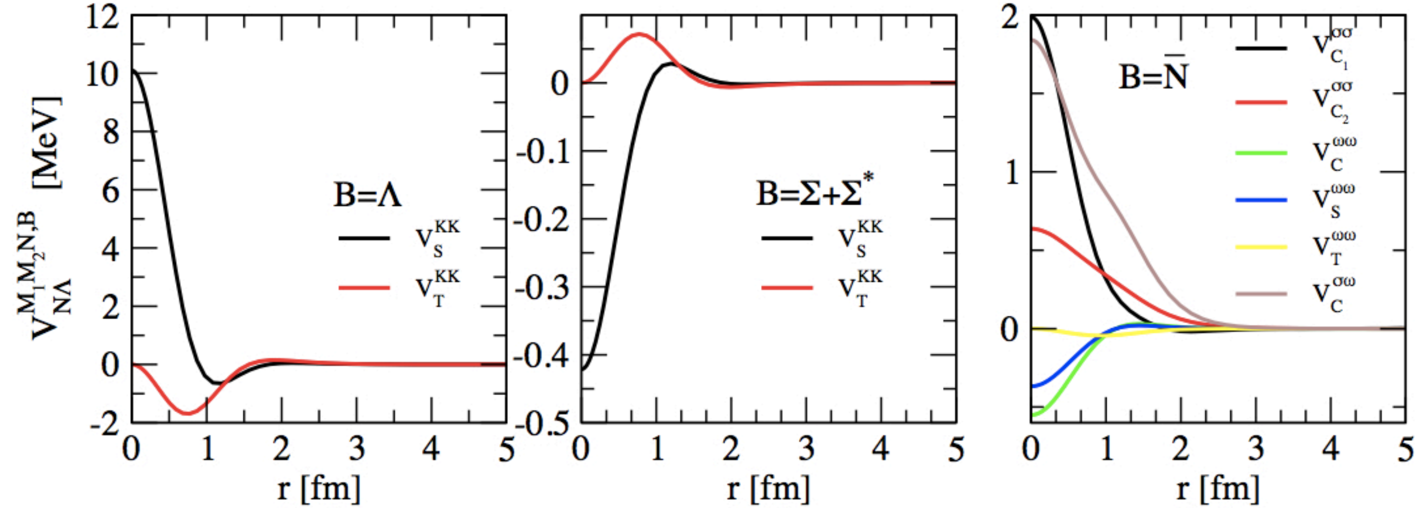

- $V_{N\Lambda}^{KKN,\Lambda}(\vec{r}) = C_{NN\Lambda}^{KK,\Lambda}\rho_N\left[V_S^{KK}(\vec{r})\vec{\sigma}_1\cdot\vec{\sigma}_2 + V_T^{KK}(\vec{r})S_{12}(\hat{r})\right]$
- $V_{N\Lambda}^{KKN,\Sigma/\Sigma^*}(\vec{r}) = C_{NN\Lambda}^{KK,\Sigma/\Sigma^*}\rho_N\left[V_S^{KK}(\vec{r})\vec{\sigma}_1\cdot\vec{\sigma}_2 + V_T^{KK}(\vec{r})S_{12}(\hat{r})\right]\vec{\tau}_1\cdot\vec{1}_2$
- $V_{N\Lambda}^{\sigma\sigma N,\bar{N}}(\vec{r}) = C_{NN\Lambda}^{\sigma\sigma,\bar{N}}\left[\rho_\Lambda V_{C_1}^{\sigma\sigma}(\vec{r}) + \rho_\Lambda^{5/3}V_{C_2}^{\sigma\sigma}(\vec{r})\right]$
- $V_{N\Lambda}^{\omega\omega N,\bar{N}}(\vec{r}) = C_{NN\Lambda}^{\omega\omega,\bar{N}}\rho_N\left[V_C^{\omega\omega}(\vec{r}) + V_S^{\omega\omega}(\vec{r})\vec{\sigma}_1\cdot\vec{\sigma}_2 + V_T^{\omega\omega}(\vec{r})S_{12}(\hat{r})\right]$
- $V_{N\Lambda}^{\sigma\omega N,\bar{N}}(\vec{r}) = C_{NN\Lambda}^{\sigma\omega,\bar{N}}\rho_\Lambda V_C^{\sigma\omega}(\vec{r})$

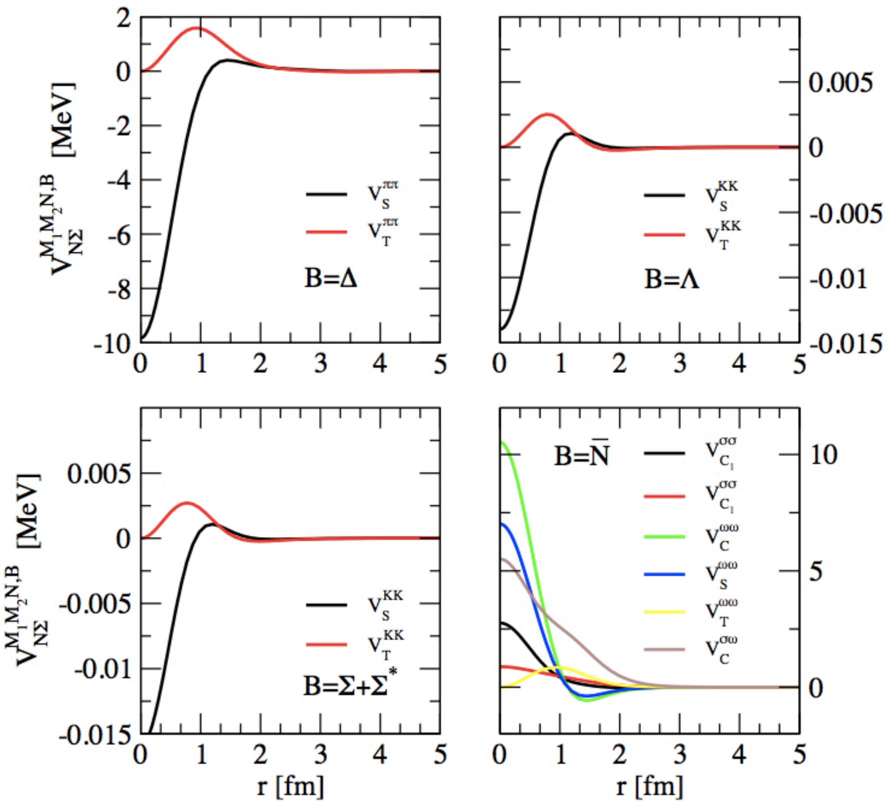

Effective NΣ density-dependent 2BF from NNΣ

- $V_{N\Sigma}^{\pi\pi N,\Delta}(\vec{r}) = C_{NN\Sigma}^{\pi\pi,\Delta}\rho_N\left[V_S^{\pi\pi}(\vec{r})\vec{\sigma}_1\cdot\vec{\sigma}_2 + V_T^{\pi\pi}(\vec{r})S_{12}(\hat{r})\right]\vec{\tau}_1\cdot\vec{I}_2$
- $V_{N\Sigma}^{KKN,\Lambda/\Sigma}(\vec{r}) = C_{NN\Sigma}^{KK,\Lambda/\Sigma}\rho_N\left[V_S^{KK}(\vec{r})\vec{\sigma}_1\cdot\vec{\sigma}_2 + V_T^{KK}(\vec{r})S_{12}(\hat{r})\right]\vec{\tau}_1\cdot\vec{\tau}_2$
- $V_{N\Sigma}^{KKN,\Sigma^*}(\vec{r}) = C_{NN\Sigma}^{KK,\Sigma^*}\rho_N\left[V_S^{KK}(\vec{r})\vec{\sigma}_1\cdot\vec{\sigma}_2 + V_T^{KK}(\vec{r})S_{12}(\hat{r})\right]\vec{\tau}_1\cdot\vec{1}_2$
- $V_{N\Sigma}^{\sigma\sigma N,\bar{N}}(\vec{r}) = C_{NN\Sigma}^{\sigma\sigma,\bar{N}}\left[\rho_\Sigma V_{C_1}^{\sigma\sigma}(\vec{r}) + \rho_\Sigma^{5/3}V_{C_2}^{\sigma\sigma}(\vec{r})\right]$
- $V_{N\Sigma}^{\omega\omega N,\bar{N}}(\vec{r}) = C_{NN\Sigma}^{\omega\omega,\bar{N}}\rho_N\left[V_C^{\omega\omega}(\vec{r}) + V_S^{\omega\omega}(\vec{r})\vec{\sigma}_1\cdot\vec{\sigma}_2 + V_T^{\omega\omega}(\vec{r})S_{12}(\hat{r})\right]$
- $V_{N\Sigma}^{\sigma\omega N,\bar{N}}(\vec{r}) = C_{NN\Sigma}^{\sigma\omega,\bar{N}}\rho_\Sigma V_C^{\sigma\omega}(\vec{r})$

Effective density-dependent transition NΣ – NΛ from NNΣ – NNΛ

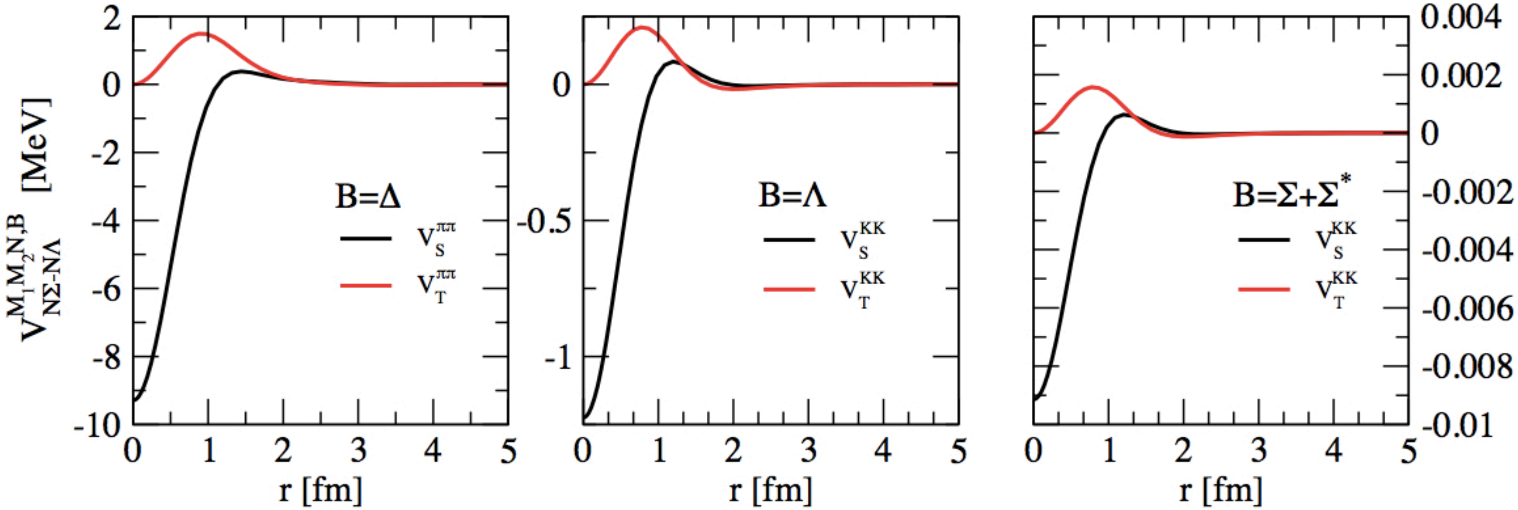

- $V^{\pi\pi N,\Delta}_{N\Sigma\leftrightarrow N\Lambda}\left(\vec{r}\right) = C^{\pi\pi,\Delta}_{NN\Sigma\leftrightarrow NN\Lambda}\rho_N\left[V_S^{\pi\pi}\left(\vec{r}\right)\vec{\sigma}_1\cdot\vec{\sigma}_2 + V_T^{\pi\pi}\left(\vec{r}\right)S_{12}\left(\hat{r}\right)\right]\vec{\tau}_1\cdot\vec{I}_2$
- $V^{KKN,\Lambda/\Sigma/\Sigma^*}_{N\Sigma\leftrightarrow N\Lambda}\left(\vec{r}\right) = C^{KK,\Lambda/\Sigma/\Sigma^*}_{NN\Sigma\leftrightarrow NN\Lambda}\rho_N\left[V_S^{KK}\left(\vec{r}\right)\vec{\sigma}_1\cdot\vec{\sigma}_2 + V_T^{KK}\left(\vec{r}\right)S_{12}\left(\hat{r}\right)\right]\vec{\tau}_1\cdot\vec{1}_2$

Effect of TBF on Mean Field & E/A

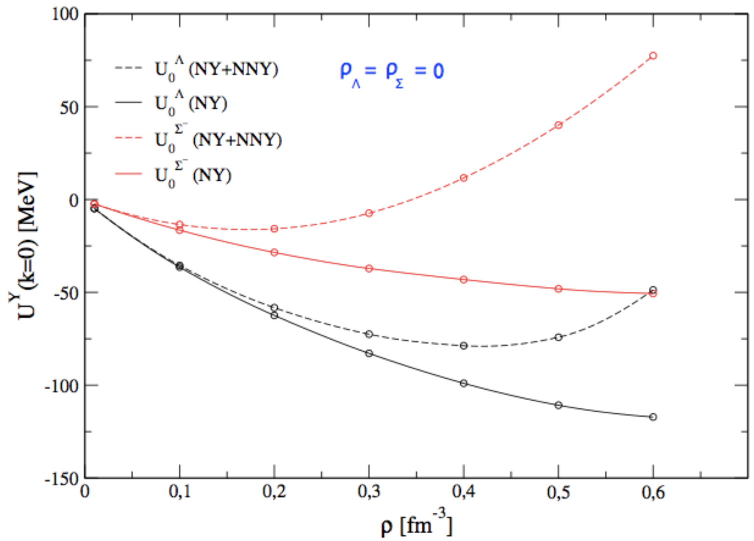

- ✓ Only NNY considered (preliminar)
- ✓ Repulsion at high densities due to Z-diagram contribution as in NNN

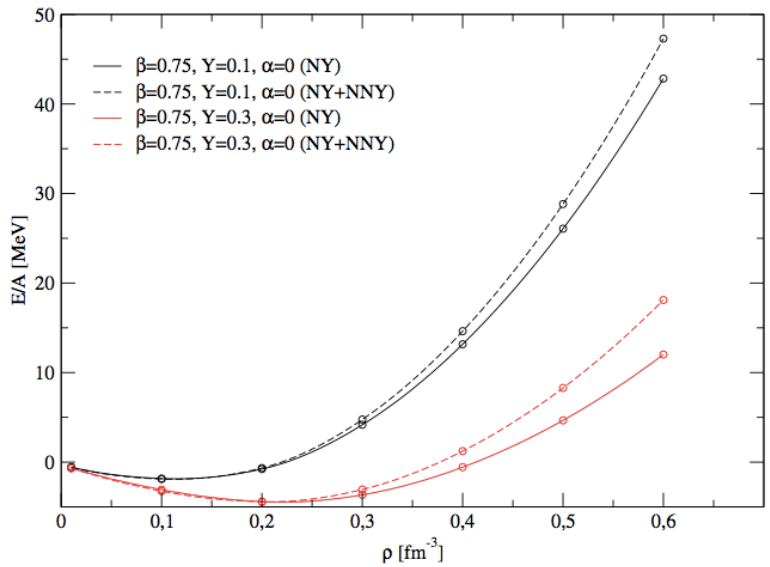

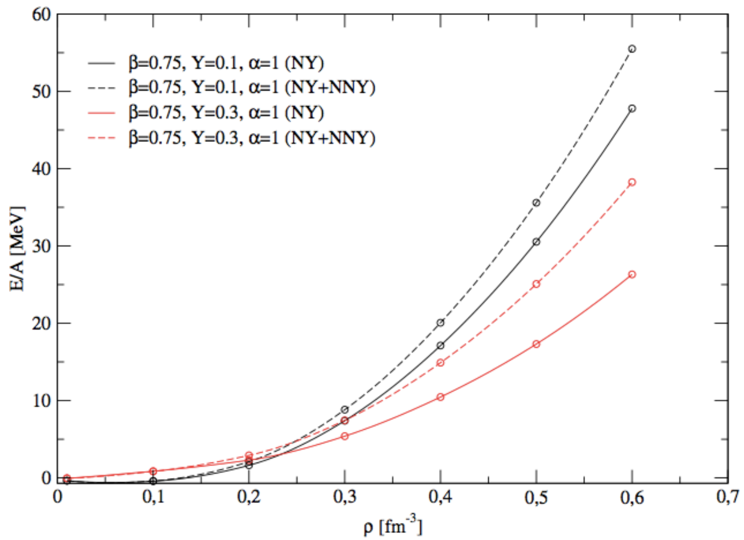

Work is in progress, many more contributions have to be considered, but we can still try to estimate the effect of hyperonic TBF in NS

1-. Construct the hyperonic matter EoS within the BHF at 2 body level (Av18 NN + NSC89 YN)

2-. Add simple phenomenological density-dependent contact terms that mimic the effect of TBF.

Density-dependent contact terms: (Balberg & Gal 1997)

Potential of a baryon B_y in a sea of baryons B_x of density ρ_x

$$V_y(\rho_x) = a_{xy}\rho_x + b_{xy}\rho_x^{\gamma_{xy}}$$

attraction

repulsion

larger than 1

Folding $V_y(\rho_x)$ with ρ_x, $V_x(\rho_y)$ with ρ_y and combining with weight factors ρ_x/ρ and ρ_y/ρ

$$\varepsilon_{xy}(\rho_x,\rho_y) = a_{xy}\rho_x\rho_y + b_{xy}\rho_x\rho_y\left(\frac{\rho_x^{\gamma_{xy}} + \rho_y^{\gamma_{xy}}}{\rho_x + \rho_y}\right)$$

Then, we have …

$$
\varepsilon_{CT} = a_{NN}\rho_N^2 + b_{NN}\rho_N^{\gamma_{NN}}
$$

$$
+a_{\Lambda N}\rho_\Lambda\rho_N + b_{\Lambda N}\rho_\Lambda\rho_N\left(\frac{\rho_\Lambda^{\gamma_{\Lambda N}} + \rho_N^{\gamma_{\Lambda N}}}{\rho_\Lambda + \rho_N}\right)
$$

$$
+a_{\Sigma N}\rho_\Sigma\rho_N + b_{\Sigma N}\rho_\Sigma\rho_N\left(\frac{\rho_\Sigma^{\gamma_{\Sigma N}} + \rho_N^{\gamma_{\Sigma N}}}{\rho_\Sigma + \rho_N}\right)
$$

$$
\rho_N = \rho_n + \rho_p\,, \quad \rho_\Sigma = \rho_{\Sigma^-} + \rho_{\Sigma^0} + \rho_{\Sigma^+}
$$

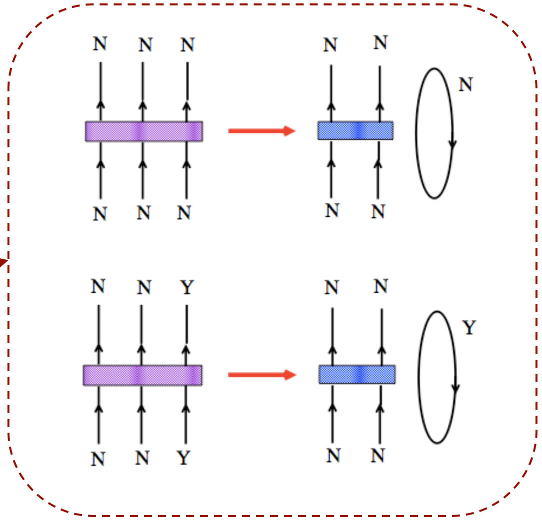

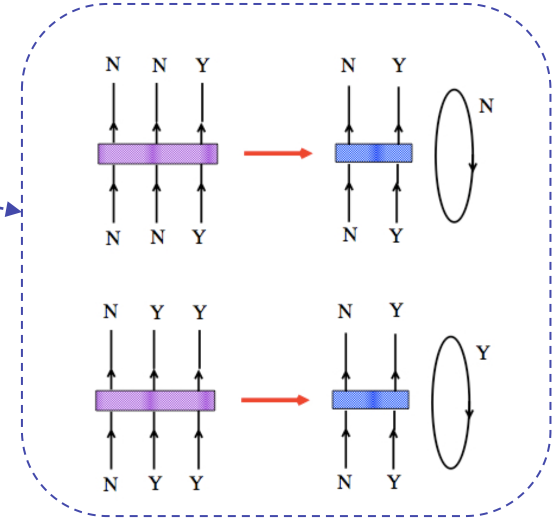

NYY ➔ YY and YYY ➔ YY
not included for consistency

The parameters a_{NN}, b_{NN} and γ_{NN} fitted to reproduce ρ_0=0.16 fm^{-3}, E/A=-16 MeV and K =211-285 MeV

γ_{NN}	a_{NN} [MeV fm^3]	b_{NN} [MeV fm$^{3\gamma_{NN}}$]	K_∞ [MeV]
2	−33.44	213.02	211
2.5	−22.08	355.03	236
3	−16.40	665.68	260
3.5	−12.99	1331.36	285

For simplicity, we take $a_{\Lambda N}=a_{\Sigma N}$, $b_{\Lambda N}=b_{\Sigma N}$ and $\gamma_{\Lambda N}=\gamma_{\Sigma N}$ with

$$a_{\Lambda N} = x a_{NN}\,, \quad b_{\Lambda N} = x b_{NN}\,, \quad x = 0, \frac{1}{3}, \frac{2}{3}, 1$$

to explore different strength of the hyperonic TBF

$\gamma_{\Lambda N}$ is obtained using the value of -28 MeV for the binding energy of a Λ in nuclear matter

$$\left(\frac{B}{A}\right)_\Lambda = 28MeV = -U_\Lambda(k=0) - a_{YN}\rho_0 - b_{YN}\rho_0^{\gamma_{YN}}$$

$$U_\Lambda(k=0) = -30.8MeV$$

Effect of hyperonic TBF on M_{max}

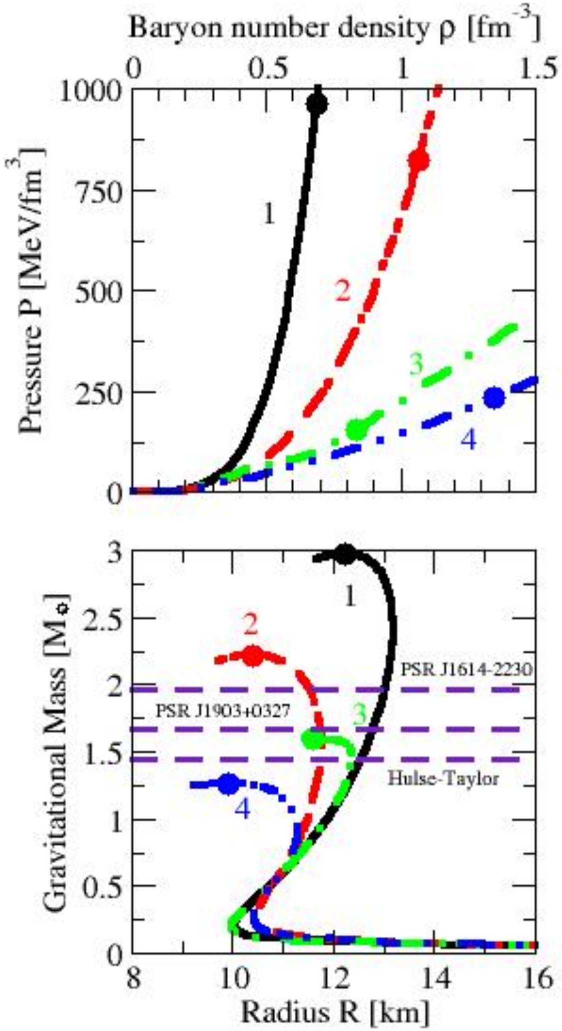

γ_{NN}	x	γ_{YN}	Maximum Mass
2	0	-	$\boxed{1.27}$ $\boxed{(2.22)}$
	1/3	1.49	1.33
	2/3	1.69	1.38
	1	1.77	1.41
2.5	0	-	1.29 (2.46)
	1/3	1.84	1.38
	2/3	2.08	1.44
	1	2.19	1.48
3	0	-	1.34 (2.72)
	1/3	2.23	1.45
	2/3	2.49	1.50
	1	2.62	1.54
3.5	0	-	1.38 $\boxed{(2.97)}$
	1/3	2.63	1.51
	2/3	2.91	1.56
	1	3.05	$\boxed{1.60}$

Hyperonic TBFs seem not to be the full solution of the "Hyperon Puzzle", although they probably contribute to its solution

$$1.27 < M_{\max} < 1.6 M_{\odot}$$

IV, Logoteta, et al., (2011)

Summary & Conclusions

- Construction of two-meson exchange hyperonic TBF

  Repulsion is obtained at high densities (Z-diagram)

  D. Logoteta, Ph.D. Thesis (Univ. Coimbra 2013)

- Simple model to establish numerical lower and upper limits to the effect of hyperonicTBF on the maximum mass of NS.

  Assuming the strength of hyperonic TBF ≤ nucleonic TBF:

  $\boxed{1.27\ M_\odot < M_{max} < 1.60\ M_\odot}$ compatible with 1.4-1.5 $M_\odot$

  but incompatible with observation of very massive NS

  PSR J1903+0327 (1.67±0.01) $M_\odot$
  PSR J1614-2230 (1.97±0.04) $M_\odot$
  PSR J0348+0432 (2.01±0.04) $M_\odot$

Take away message

Hyperonic Three-Body Forces seem not to be the full solution to the "Hyperon Puzzle", although they probably can contribute to it

- You for your time & attention
- The organizers for their invitation
- The sponsors for their support

COMPETE
PROGRAMA OPERACIONAL FACTORES DE COMPETITIVIDADE

comp star